MICROCOPY RESOLUTION TEST CHART

NATIONAL BUREAU OF STANDARDS

aval Research Laboratory

shington, DC 20375-5000

DTIC FILE COPY

Computer Modeling for Optical Waveguide Sensors

J. F. GIULIANI AND P. P. BEY, JR.

Surface Chemistry Branch
Chemistry Division

DTIC
ELECTE
JAN 1 1 1988
S D
D

December 15, 1987

REPORT DOCUMENTATION PAGE

1a REPORT SECURITY CLASSIFICATION UNCLASSIFIED		1b RESTRICTIVE MARKINGS *AI877O2*
2a. SECURITY CLASSIFICATION AUTHORITY		3 DISTRIBUTION AVAILABILITY OF REPORT
2b. DECLASSIFICATION / DOWNGRADING SCHEDULE		Approved for public release; distribution unlimited.
4 PERFORMING ORGANIZATION REPORT NUMBER(S) NRL Memorandum Report 6071		5 MONITORING ORGANIZATION REPORT NUMBER(S)

6a. NAME OF PERFORMING ORGANIZATION Naval Research Laboratory	6b OFFICE SYMBOL (If applicable)	7a NAME OF MONITORING ORGANIZATION
6c. ADDRESS (City, State, and ZIP Code) Washington, DC 20375-5000		7b ADDRESS (City, State, and ZIP Code)

8a. NAME OF FUNDING / SPONSORING ORGANIZATION	8b. OFFICE SYMBOL (If applicable)	9 PROCUREMENT INSTRUMENT IDENTIFICATION NUMBER

8c. ADDRESS (City, State, and ZIP Code)	10 SOURCE OF FUNDING NUMBERS			
	PROGRAM ELEMENT NO	PROJECT NO	TASK NO	WORK UNIT ACCESSION NO

11. TITLE (Include Security Classification)

Computer Modeling for Optical Waveguide Sensors

12. PERSONAL AUTHOR(S)
Giuliani, J.F. and Bey, Jr., P.P.

13a. TYPE OF REPORT Interim	13b TIME COVERED FROM 6/86 TO 1/87	14 DATE OF REPORT (Year, Month, Day) 1987 December 15	15 PAGE COUNT 26

16 SUPPLEMENTARY NOTATION

17 COSATI CODES			18 SUBJECT TERMS (Continue on reverse if necessary and identify by block number)
FIELD	GROUP	SUB-GROUP	Optical waveguide sensors
			Computer modeling

19 ABSTRACT (Continue on reverse if necessary and identify by block number)

A two-layer model for the analysis of an optical waveguide chemical vapor sensor is developed using a program written for a low cost (PC) computer, which takes into account a non-adsorbing glass/fluid interface, the number of optical reflections, and probe beam divergence, for angles of incidence which are skewed about the critical angle for total internal reflection. This model is applied in the analysis of condensed organic vapors employing an uncoated optical thin-walled glass capillary device developed at NRL. Reasonable agreement is obtained between the experimental results and model predictions.

20 DISTRIBUTION/AVAILABILITY OF ABSTRACT X UNCLASSIFIED/UNLIMITED ☐ SAME AS RPT ☐ DTIC USERS	21 ABSTRACT SECURITY CLASSIFICATION UNCLASSIFIED
22a NAME OF RESPONSIBLE INDIVIDUAL Dr. John F. Giuliani	22b TELEPHONE (Include Area Code) (202) 767-1399 Code 6170

DD Form 1473, JUN 86 *Previous editions are obsolete.*

CONTENTS

Computer Modeling for Optical Waveguide Sensors

INTRODUCTION

The development and application of optical waveguide and fiber optic sensors for detecting toxic gases and more recently biologicals have rapidly expanded over the last several years. Much of the interest stems from their geometrical simplicity, relatively inexpensive starting materials (i.e. glasses, polymers), rapid response to physical and chemical changes, freedom from electrical interference, and their adaptability to micro-electronic fabrication techniques.

For the past five years NRL has been developing a number of waveguide chemical sensors for detecting toxic vapors and other gases [1-6].

More recently, this waveguide sensor has been adapted to liquid phase bio-chemical applications, with particular emphasis on antigen-antibody competitive binding immuno assay surface interactions [7].

Although optical waveguide sensors can take various geometric forms, we have adopted the hollow cylindrical glass structures as our basic device design. Figure 1 shows a picture of the hollow cylindrical waveguide sensor structure together with an LED light source and photo detector.

The main advantages of this structure are its ruggedness and economy of size, in which the number of total internal optical

1

CAPILLARY TUBE

LIGHT EMITTING DIODE

PHOTOTRANSISTOR

CM
1   2   3   4   5   6   7
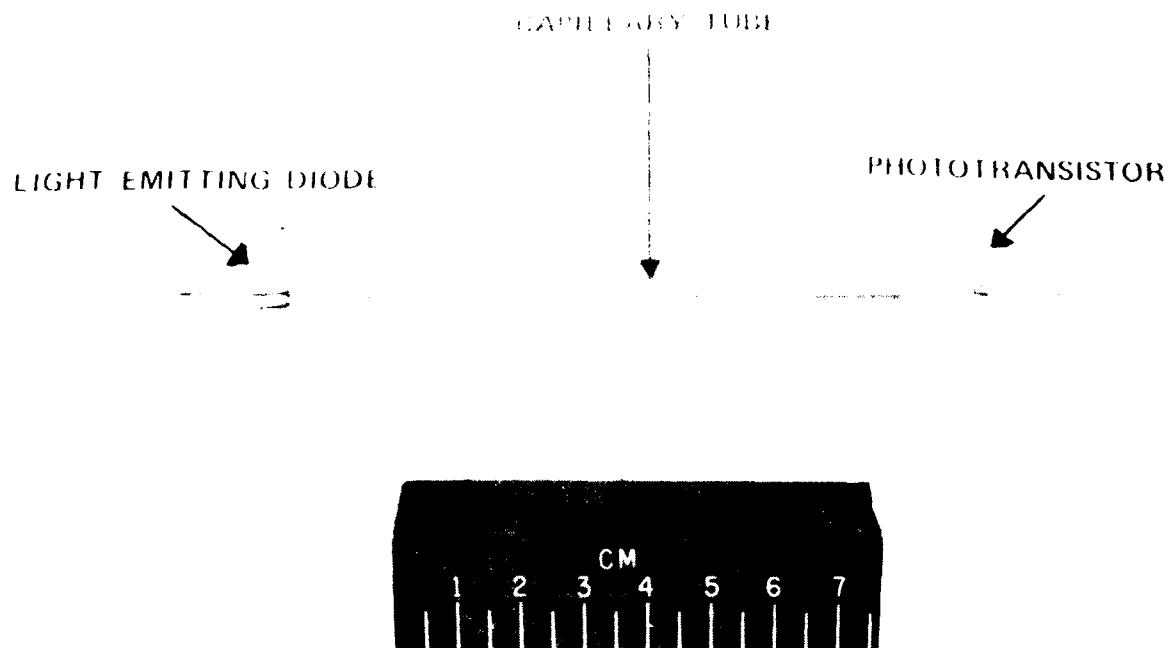
Figure 1.   Optical Waveguide Capillary Sensor Incorporating
            an LED Light Probe and Photo Transistor

reflections for this 90 mm x 1.1 mm (o.d.) X 0.8 mm (i.d.) glass

tube is approximately 300.   Moreover, one end of this cylindrical

structure is formed into a lens-like curved surface for efficient

focusing of the multiply reflected probe beam into a small

photo detector.[1].   Down the center of this hollow cylinder is

inserted an optical stop, which prevents collinear background

stray light from interfering with the multiply reflected light

inside the thin (0.3mm) glass wall of the cylinder.   This

geometry produces what has been termed "hollow cone" illumination

into the waveguide structure.   Kapany and Pontarelli, [8] have

shown that this form of illumination gives rise to high

fractional sensitivity for detecting very small changes in

refractive index at the waveguide surface, when compared with a
solid rod illumination configuration.

The work reported here involves the use of a computer
program for modeling the transmission of an unpolarized light
probe beam which is totally internally reflected at a non-
absorbing glass/fluid interface. The analysis takes into account
the probe beam divergence, and the number of optical reflections
for various ranges of incidence angles about the critical angle
for total internal reflection. The resultant probe beam
transmission may be plotted as a function of changes in the
refractive index of the surrounding fluid medium.

BASIC EQUATIONS

Figure 2 represents schematically a section of the capillary
waveguide structure, which, depicts the principal incident light
rays emitted from an unpolarized LED light source coupled into
the open end of the capillary tube. θ_{cr} is the critical angle
for total internal reflection, θ_i is the angle of incidence, for
an angular spread θ_1, θ_2 and the "dark" region in the schematic
represents an optical stop which is inserted to exclude paraxial
light rays from interfering with the totally reflected rays. The
heavy line indicates a ray at θ_i, which is coupled into the
waveguide and after N optical reflections can be coupled out into
a photo detector, which measures the transmission (T) as sensed
by the light probe at the glass/fluid interface down the length
of the cylinder. For the situation in which the waveguide and the
surrounding fluid are non-absorbing, the waveguide transmission
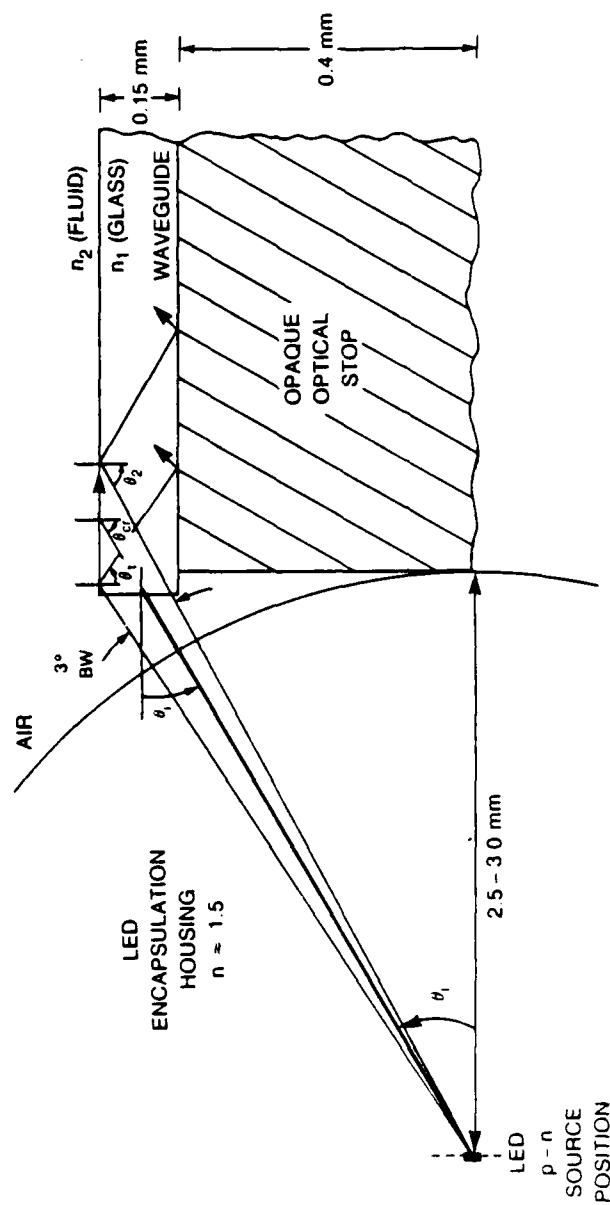(T) is given by [9].

$$T = {}^{N}$$

Figure 2. Light rays entering the glass wall of a capillary waveguide from a light-emitting diode. The heavy ray illustrates the behavior of one specific ray at θ_1 which approaches glass fluid interface, at the critical angle. The dark area represents an optical stop, placed inside the hollow cylinder.

where the reflectivity $\rho = \dfrac{1}{2}\left[\left(\dfrac{\sin\ (\theta-\phi)}{\sin\ (\theta+\phi)}\right)^2 + \left(\dfrac{\tan\ (\theta-\phi)}{\tan\ (\theta+\phi)}\right)^2\right]$ for $\phi < 90^\circ$

and $\rho = 1$ (otherwise)

N is the number of optical reflections and θ, ϕ are the angles of incidence and refraction, respectively, at the interface between the waveguide and the less dense surrounding fluid medium (i.e. gas or liquid). If the indices of refraction of the waveguide and surrounding fluid medium are n_1 and n_2, respectively, then by Snell's Law:

$$n_1 \sin \theta = n_2 \sin \phi$$

and $\theta_{cr} = \sin^{-1}\left[\dfrac{n_2}{n_1}\right]$ when $\phi = 90^\circ$ \qquad (2)

Equation (1) may be re-written to take into account the experimental situation for a diverging uniformly illuminating light source and for a range of angles of incidence below and above the critical angle for total internal reflection. Thus, the transmission then takes the form:

$$T = \dfrac{\int_{\theta_1}^{\theta_{cr}} \rho^N d\theta + (\theta_2 - \theta_{cr})}{(\theta_2 - \theta_1)} \qquad (3)$$

where $\theta_2 - \theta_{cr}$ is a range of angles of incidence above the critical angle, and $\theta_2 - \theta_1$ is the total angular spread of all angles of incidence about the critical angle θ_{cr}. It should be noted that $\underset{\sim}{N}$ in equation (3) is a function of θ, since

$$\phi = \sin^{-1}\left[\frac{n_2}{n_1} \sin \theta\right] , \text{ see equation } (2)$$

Thus equation (3) describes the general experimental situation, which is schematically shown in Figure 2.

Equation (3) may be evaluated numerically by using a micro-computer. The program employed in this transmission analysis is written in basic language, and is listed at the end of this report in the appendix.

COMPUTER MODELING ANALYSIS

The following series of Figures 3 to 5, summarize the computer modeling for a glass waveguide of refractive index, n_1 = 1.50, whose surface is in contact with a liquid of varying refractive index, n_2 between 1.320 and 1.340.

The resultant transmissions are plotted as a function of the change in refractive index of the liquid, under a variety of experimental conditions, which include probe beam divergence or beam spread (BW), the number of optical reflections (N), and for incident angles skewed about the critical angle.
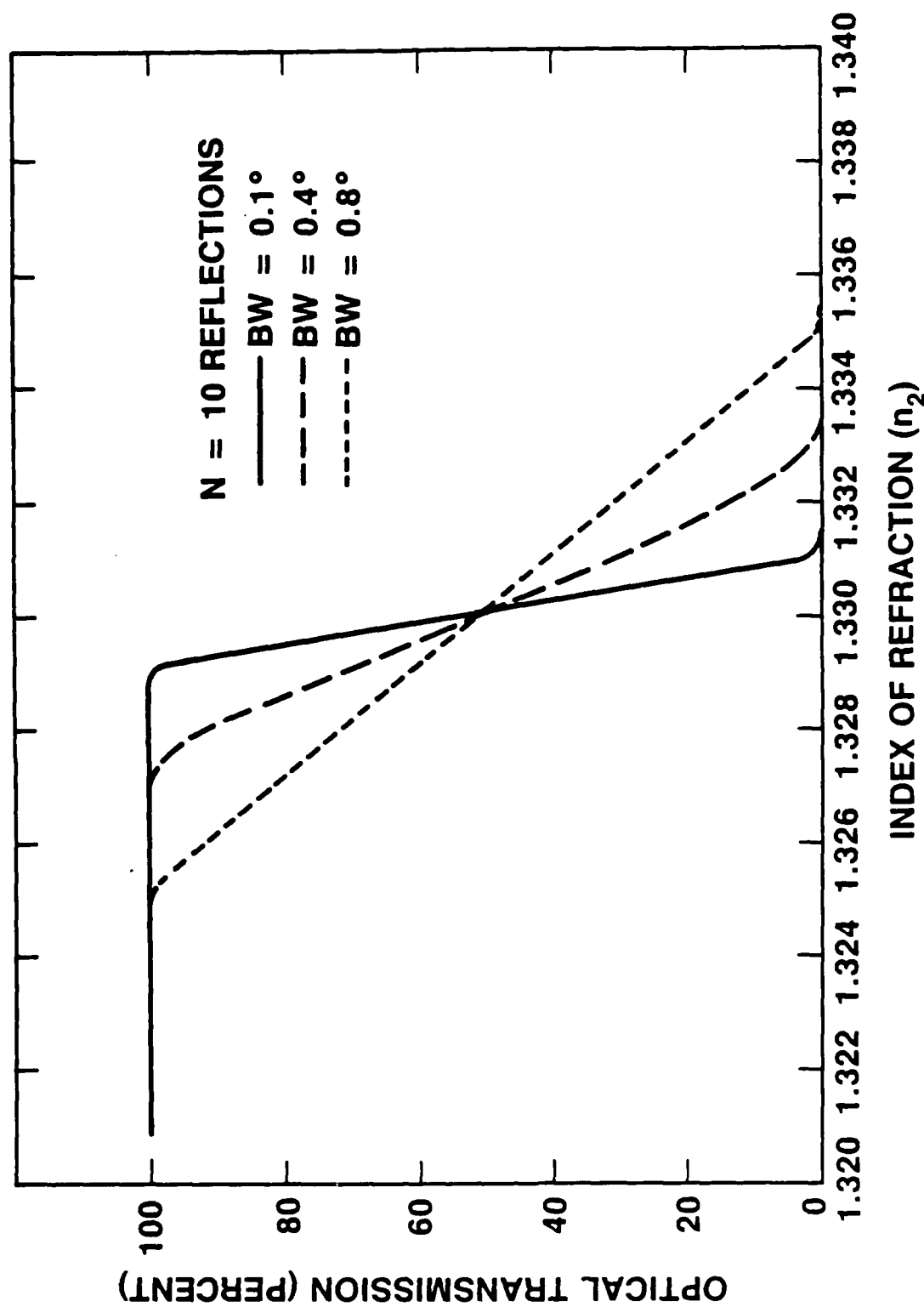
Figure 3. Optical transmission plotted against n_2 for a series of divergent probe beams. Note, that the smaller the beam divergence the steeper the slope, and hence the greater the differential sensitivity. Also, the beam divergence shifts the critical angle.

Figure 3 is a plot of the integrated transmission with change in refractive index of the liquid, for 10 optical reflections, and for a set of diverging probe beams, whose beam widths are 0.1°, 0.4° and 0.8°. The angle of incidence θ_i is set equal to the critical angle corresponding to $n_2 = 1.33$. As the index of refraction of the liquid decreases, the optical transmission increases rapidly as n_2 approaches 1.33. The steepness of the slope is a measure of the index of refraction resolution and hence the device sensitivity. It is readily seen, that the least divergent probe beam (ie. BW = 0.1°) gives the highest resolution. Also, the change in index of refraction for the range from zero to 100 percent transmission, is significantly greater with increasing beam spread. It is interesting to note that all three curves intersect at a transmission of 50%. This effect can be understood by an inspection of Equation (3), in which the integrated function contributes very little to changes in the transmission for the case of a uniformly illuminating probe beam whose beam spread is symmetric about the critical angle for 10 optical reflections. Recalling the sketch shown in Figure 2 for a symmetric spread of angles θ_1, θ_2 about θ_{cr}, where $\theta_2 - \theta_{cr} \approx \dfrac{\theta_2 - \theta_1}{2}$ and for 10 reflections.

$$T \approx \frac{\theta_2 - \theta_{cr}}{\theta_2 - \theta_1} = \text{ 1/2 or 50\%.}$$
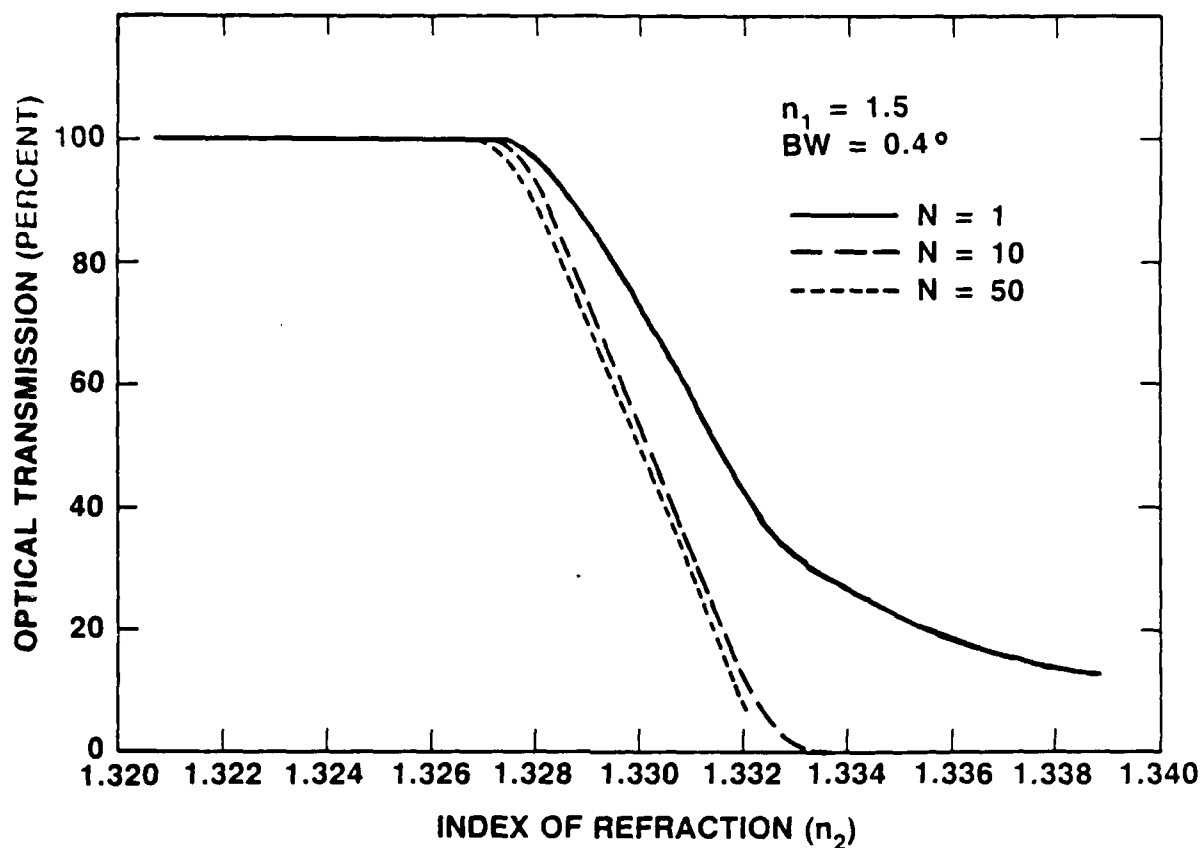
Figure 4. Optical transmission versus n_2 as a function of N number of optical reflections. Note that above 10 reflections no significant slope change occurs.

An important factor in assessing optical waveguide sensors is the optimal number of total internal optical reflections required to give the best refractive index resolution. Figure 4 gives a computer plot of transmission versus n_2 for a set of optical reflections N, from 1 to 50, for a probe beam of 0.4° beam spread, and for θ_{cr} equal to 62.46° corresponding to n_2 = 1.330. As can be easily seen from the different slopes, a single reflection i.e. N = 1, gives the poorest device sensitivity. Not until N = 10 reflections does the device sensitivity increase significantly as indicated by the steeper slope. However, for reflections from N equal to 10 to N equal to 50, no apparent slope change is evident. This saturation can be understood by

9

considering the angles of incidence θ_1 to θ_2 within the beam
width. Thus, angles of incidence θ_i less than the critical angle
θ_{cr}, contribute relatively more i.e., see equation (3) to the
total reflectivity (or transmission), for a small number of
reflections. As the total number of reflections increases above
10, only those light rays which come close to the critical angle
are transmitted, that is significantly fewer rays, whose angles
of incidence are less than the critical angle, $(\theta_1 < \theta_i < \theta_{cr})$
contribute to the total transmission. Another practical case
relating to optical waveguide detection sensitivity, involves
the general experimental situation in which the initially fixed
incident beam can be angularly modulated due to relatively small
refracture index gradients set up in the fluid layer above the
glass surface. A simulated computer analysis for this case is
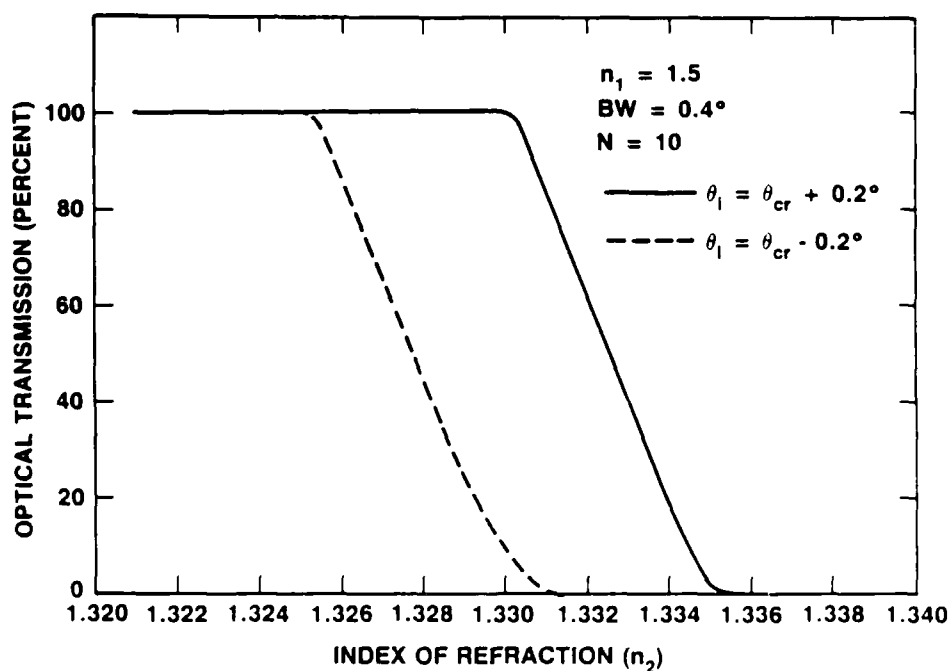shown in Figure 5.

Figure 5. Optical transmission versus n_2 for angles of
incidence skewed to ± 0.2 about the critical angle.

Here, the optical transmission is plotted versus index n_2 for angles of incidence which are dynamically skewed $\pm$ 0.2° away from the critical angle (θ_{cr}) corresponding to n_2 = 1.33. For this case, the transmission is calculated for a probe beam spread of 0.4°, and for 10 optical reflections. The solid curve denotes incident angles skewed +0.2° above the θ_{cr}, and the dashed curve refers to those incident angles skewed -0.2° below θ_{cr}. Although the shapes of these two curves are relatively unaffected, as noted by the similar slopes, nontheless, a fluctuation of $\pm$ 0.2° at the dynamic fluid/glass boundary layer, does produce a significant modulation of nearly 100 percent output in detected waveguide transmission. Hence, even with a fixed angle of incidence of the light source coupled into the waveguide structure, dynamic surface effects at the glass/fluid boundary can significantly modify the angles of incidence at this boundary and these refractive index variations can be exploited to detect small changes in the optical properties of such a fluid layer. In summarizing this section, the modeling analysis clearly shows that to obtain high differential sensitivity for an optical waveguide chemical sensor, the light source must have a low beam divergence, the angle of incidence should be as close to the critical angle as possible, and up to 10 optical reflections are required for maximizing the slope sensitivity.

DISCUSSION

The computer analysis discussed in the previous section can be applied to the NRL "hollow-cone" illumination glass waveguide vapor sensor, to predict its sensitivity, using a commercial red 660 nm LED source as the probe beam. The experiment consisted in

measuring changes in the optical transmission at 660 nm as a function of a series of indices of refraction, obtained from condensing on the waveguide surface, vapors of several organic compounds and water of known indices of refraction. These vapors were produced by bubbling dry nitrogen into a flask containing the liquid compound to be tested, and admitting the vapor/nitrogen carrier gas into a 0.1ml dead volume chamber, into which the waveguide sensor is immersed. At a fixed vapor/gas flow rate of 0.06 liters/min. at room temperature, and at atmospheric pressure, the saturated vapors from a particular sample compound, was allowed to condense onto the glass surface of the uncoated capillary. After a few seconds duration, a measurable stable voltage shift relative to the nitrogen carrier gas baseline voltage was detected. The measured change in voltage is directly proportional to a change in transmission relative to the nitrogen carrier gas. The procedure for detecting condensed vapors on the waveguide surface has been published in detail elsewhere [1,2].

Figure 6 displays the NRL waveguide capillary measured transmission versus index of refraction for a range of values from, benzene (1.5012) to water (1.3330) under the previously described experimental conditions. The solid circles are the measured voltages readings expressed as percent transmission relative to air. The error bars represent the standard deviation limits for several runs per vapor. The solid curve drawn through these points represents the best fit by our computer semi-infinite two-layer model, assuming a critical angle of about 82.5°, and using the measured beam spread of the LED into the
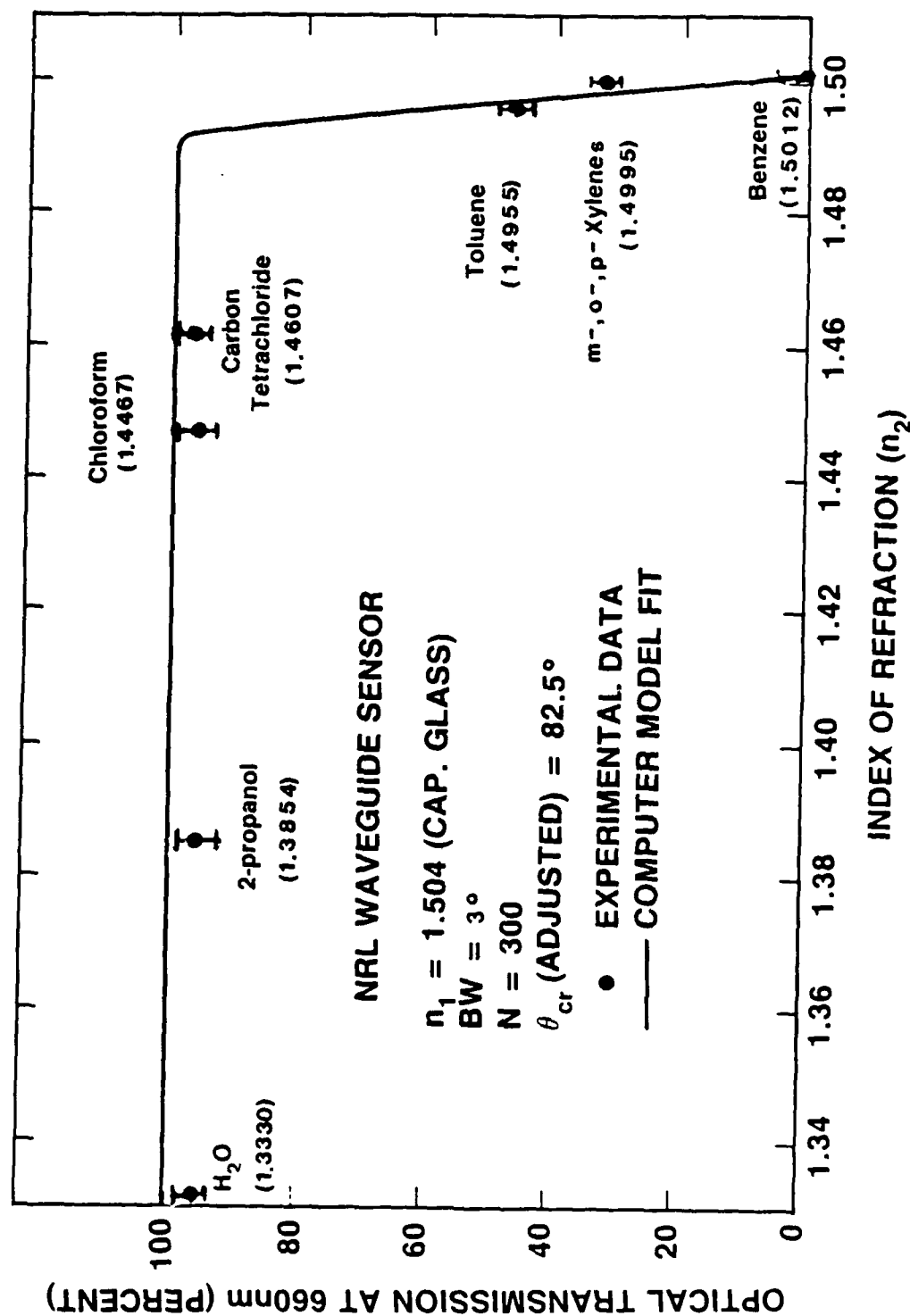
12

Figure 6.   NRL optical waveguide transmissions at 660 nm, measured over a range of refractive indices obtained from condensed vapors. Computer fit was made based on measured device parameters, such as beam spread, and the number of effective reflections.

waveguide of 3°, and 300 optical reflections, as computed from the length to glass wall diameter ratio (i.e. 9cm/0.3mm/= 300). The important point to note here is that the data points appear to correlate well with the shape of the two-layer model prediction. Unfortunately, no readily available organic compounds were found which have accurately measured refractive indices above and below the "knee" of the theoretical curve shown in Figure 6. Nevertheless, an approximate differential slope sensitivity $1/T(\Delta T/\Delta n_2) \approx 340 \pm 25\%$ is obtained from the experimental data between indices 1.5012 (benzene) and 1.4955 (toluene), where ΔT is the measured transmittance difference between toluene (T = 47%) and benzene (T = 0.5%), and the average transmission T between toluene and benzene is 24%. Consequently, if for example, two organic fluid species have indices of refraction which differ by 5 parts in 10^5, (i.e. $\Delta n_2 = 5 \times 10^{-5}$), and fall on the rapidly decreasing slope as, shown in Figure 6, then the change in transmittance (ΔT) required to be detected by the waveguide sensor ($\Delta T\%/\Delta n_2$) is $8158 \times 5 \times 10^{-5} = 0.4\%$.

To determine the present NRL optical sensor differential sensitivity, a separate experiment was performed using the same device and electronics in a static calibration mode. Here, the calibration consisted in adjusting the angle of incidence by positioning the LED housing at the proper distance from the open end of the capillary and monitoring the intensity with a photodetector. When the measured output intensity from the capillary is a maximum, then the incident angle equals the critical angle. The critical angle in the air for this case is $\theta_{cr} = 41.8°$. This setting ensured

nearly 100% transmission of the 660 nm LED through the waveguide device. The transmitted light detected by the red sensitive phototransistor produced a voltage of 1000 mV on a standard DC chart recorder, after amplification. Next, a set of calibrated neutral density filters, ranging in attenuation between 1.0 OD and 3.0 OD were placed in front of the LED source. Hence the transmission could be varied between 100% and 0.1%. The corresponding measured voltages ranged between 1000 mV and 1 mV, and fall on a staight-line plot of transmission versus voltage. The measurement voltage error is approximately ±1 percent. Hence, a 0.5% change in optical transmission gives a readily measurable voltage of 5mV, and therefore, indicates that a change in refractive index of 5 parts in 10^5 should be readily detectable by this sensor, assuming no scattering losses.

A further verification of the reliability of the computer model can be made by working backwards from the assumed critical angle (82.5°) to the calculation of the angle of incidence coupled into the 0.3mm thick capillary wall. Referring to the sketch shown in Figure 2, if θ_{cr} is 82.5°, then the computed angle of incidence, applying Snell's Law for an incident ray θ_i at the air/glass interface, give a calculated $\theta_i \approx 11°$. This angle is in reasonable agreement with the measured values of the order of 8° to 10°, for this LED divergent beam/capillary aperture sensor geometry. The measured distance between the LED source element and the open capillary input surface is about 2.5 mm to 3.0 mm, and the total external beam width intercepted by the capillary input aperture is approximately 3°.

It should be noted at this point, that at first glance, our two-layer single boundary model should not be applicable to the experimental data shown in Figure 6. Here, the condensed fluid layer in fact, does have a second boundary (i.e. fluid/air interface) due of course to a finite fluid thickness. If a second interface were important in this dynamic equilibrium flow experiment, then it should manifest itself, for example, by giving rise to a high reflectivity for liquids which have refractive indices corresponding to the critical angles below that depicted in Figure 6, but greater than the critical angles at the second boundary. Particularly, for the case of benzene, whose refractive index nearly equals that of glass, a back reflection at the fluid/air interface, should in general have produced no significant decrease in transmittance at the glass/fluid interface and hence the measured transmittance should not have decreased to almost zero. The fact that the measured transmittance for benzene does drop significantly to about zero (i.e. 0.5%), implies that the second reflecting boundary does not contribute to the measured transmission. A reasonable explanation for the negligible effect of this second interface may be related to the dynamics of the experiment in which a roughened surface layer is produced in the vapor flow over the glass surface, such that any light which gets transmitted into and back-reflected at the fluid/air boundary is effectively scattered out of the waveguide. This hypothesis was tested by reducing our normal benzene vapor flow rate from 90 mL/min to 10

mL/min, while maintaining the same vapor pressure at both flow rates. The relative transmission increased from 0.7% at 90 mL/min to 55% at 10mL/min, thus suggesting that the slower flow rate produced a less roughened scattering surface and hence a greater back reflection into the capillary glass. These results therefore indicate that unless the vapor flow is significantly larger than 10 mL/min, the interfering second boundary layer can significantly enhance the optical transmission, and hence a single boundary, two-layer model would not be applicable in the first approximation to these vapor flow experiments.

SUMMARY

A computer model has been derived for the assessment of specific factors which influence the sensitivity of waveguide chemical sensors. This analysis allows for the change in transmission of a probe beam at the glass/less dense fluid interface of varying index of refraction, to be evaluated as a function of probe beam divergence, the number of optical reflections, and for angles of incidence skewed about the critical angle for total internal reflection.

Reasonable agreement was obtained in the application of this two-layer model to a specific transmission versus refractive index experiment involving an NRL chemical vapor sensor in a dynamic equilibrium condensed vapor experiment. The initial

experimental results, taken with this optical sensor indicates, that changes in refractive index for two species (i.e. liquid or condensed vapor) which differ by five parts in 10^5 may be readily discerned, if the angle incidence of the light source is set close to the critical angle for one of the species. Finally, we had previously demonstrated [3] that coating the surface of our device with a particular dye film which is known to increase its optical density when exposed to a specific organophosphonate chemical warfare simulant, produced a measurable change in transmittance of 0.4 percent at vapor concentrations of 10 ppm.

ACKNOWLEDGMENT

OPTICAL WAVEGUIDE TRANSMISSION

MS BASIC: SOURCE LISTING:

```
10 REM DOS FILE NAME:CRANGLE
20 PI#=3.14159265#
30 CLS
40 INPUT "Disk File Name = ",NAMS:NAMS="B:"+NAMS
50 OPEN NAM$ FOR OUTPUT AS #1
60 INPUT "Number of Reflections = ",NR
70 INPUT "Index n1 = ",N1#
80 INPUT "INDEX N21 = ",N21#
90 INPUT "INDEX N22 = ",N22#
100 INPUT "Index Interval Dn2 = ",DN2#
110 INPUT "ANGLE OF INCIDENCE = ",THETAIN#
120 INPUT "Beam Spread (Degrees) = ",DISP#
130 DEF FNF#(T#)=.5*((TAN(T#-TS#)/TAN(T#+TS#))^2+(SIN(T#-TS#)/SIN(T#+TS#))^2)
140 DEF FNPHI#(Y#)=ATN(N1#*SIN(Y#)/SQR(ABS(N2#^2-(N1#*SIN(Y#))^2)))
150 EP=.1:DISP#=PI#*DISP#/180!
160 THETA1#=THETAIN#*PI#/180-DISP#/2
170 THETA2#=THETA1#+DISP#
180 N21=N21#:N22=N22#:DN2=DN2#
190 JJ=-1
200 FOR N2=N21 TO N22 STEP DN2
210 JJ=JJ+1
220 N2#=N21#+(JJ-1)*DN2#
230 IF N2#>=N1# THEN STOP
240 IF N2#=N20# THEN GOTO 260
250 N2#=N2
260 GOSUB 300
270 NEXT N2
280 CLOSE #1
290 END
300 THETAC#=ATN(N2#/SQR(N1#^2-N2#^2))
310 IF THETA1#<THETAC# THEN GOTO 330
320 RHO#=1:GOTO 420
330 X1#=THETA1#
340 IF THETAC#<THETA2# THEN GOTO 370
350 X2#=THETA2#
360 GOTO 380
370 X2#=THETAC#
380 GOSUB 450
390 IF THETAC#<THETA2# THEN GOTO 410
400 RHO#=SUM#(2)/DISP#:GOTO 420
410 RHO#=(SUM#(2)+THETA2#-THETAC#)/DISP#
420 N2=N2#:RHO=RHO#:SUM=SUM#(2):DN2=DN2#
430 PRINT JJ,RHO,SUM:WRITE #1,JJ,RHO
440 RETURN
```

```basic
430 PRINT JJ,RHO,SUM:WRITE #1,JJ,RHO
440 RETURN
450 REM DOS FILE NAME:SIMPSON
460 DEF FNLN(T#)=.4343*2*NR*LOG(T#)
470 DX#=(X2#-X1#)/4
480 N=2
490 IF THETA2#>THETAC# THEN GOTO 510
500 TS#=FNPHI#(X2#):FF#=FNF#(X2#):GOTO 520
510 FF#=1
520 TS#=FNPHI#(X1#):F1#=FNF#(X1#)
530 IF FNLN(F1#)<-35 THEN F1#=0 ELSE F1#=F1#(  NR)
540 IF FNLN (FF#)<-35 THEN FF#=0 ELSE FF#=FF#(  NR)
550 SUM12#=F1#+FF#
560 XX#=X1#+DX#:TS#=FNPHI#(XX#):T1#=FNF#(XX#)
570 IF FNLN (T1#)<-35 THEN T1#=0 ELSE T1#=T1#(2*NR)
580 XX#=X1#+3*DX#:TS#=FNPHI#(XX#):T2#=FNF#(XX#)
590 IF FNLN (T2#)<-35 THEN T2#=0 ELSE T2#=T2#(2*NR)
600 SUM1#=T1#+T2#
610 XX#=X1#+2*DX#:TS#=FNPHI#(XX#):SUM2#=FNF#(XX#)
620 IF FNLN(SUM2#)<-35 THEN SUM2#=0 ELSE SUM2#=SUM2#(2*NR)
630 SUM#(1)=(SUM12#+4*SUM1#+2*SUM2#)*DX#/3
640 SUM2#=SUM1#+SUM2#
650 N=2*N
660 DX#=DX/2
670 SUM1#=0
680 FR I1=1 TO N
690 XX#=X1#+(2*I1-1)*DX#
700 TS#=FNPHI#(XX#):FF#=FNF#(XX#)
710 IF FNLN(FF#)<-35 THEN GOTO 720 ELSE SUM 1#=SUM1#+FF#(2*NR)
720 NEXT I1
730 SUM#(2)=(SUM12#+4*SUM1#+2*SUM2#)*DX#/3
740 IF SUM#(2)<.1*ABS(THETA2#-THETAC#) THEN GOTO 770
750 IF ABS((SUM#(2)-SUM#(1))/SUM#(2))<EP THEN GOTO 770
760 SUM2#=SUM1#+SUM2#:SUM#(1)=SUM#(2):GOTO 650
770 RETURN
```

REFERENCES

1. Giuliani, J.F., Wohltjen, H., and Jarvis, N.L., _Optics Letters_, 1983, 8,54.

2. Giuliani, J.F., and Jarvis, N.L., _Sensors and Actuators_, 1984, 6, 107.

3. Giuliani, J.F. Wohltjen, H., and Jarvis, N.L., "General Theory and Design Considerations for Optical Waveguide Chemical Vapor Sensors", NRL Memorandum Report 5457, Dec. 1984.

4. Giuliani, J.F. and Jarvis, N.L., _J. Chem. Phys._, 1985, 82, 1021.

5. Ballantine, D.S. and Wohltjen, H., "An Optical Waveguide Humidity Detector", _NRL Memorandum Report 5666_, Oct. 1985.

6. Giuliani, J.F., _J. Chem. Phys.,_ 1985, 83, 5998.

7. Giuliani, J.F. and Dominguez, D., (unpublished work).

8. Kapany, N.S. and Pontarelli, D.A., _Applied Optics_, 1983, 2, 425.

9. Born, M. and Wolfe, E., "Principles of Optics," (Pergamon
   Press. Inc., New York, 1964), pp. 38-45.

END

FILMED

FEB. 1988

DTIC